The seismic responses of girder bridges with novel sliding lead rubber bearings

Yi-feng Wu[*1], Ai-qun Li [1,2] and Hao Wang [2]

[1] *School of Civil and Transportation Engineering, Beijing University of Civil Engineering and Architecture, Beijing, 100044, China*
[2] *School of Civil Engineering, Southeast University, Nanjing, 210096, China*

Abstract. Based on the commonly used lead rubber bearing (LRB) and sliding rubber bearing (SRB), a novel sliding lead rubber bearing (SLRB) is introduced. The mechanical properties of the three types of bearings were investigated by experiment. After that, a simply supported girder bridge with a 1/4 scale ratio was designed and fabricated, and the dynamic characteristics and seismic response of the bridge equipped with the above three types of bearings were studied. Results show that the girder's acceleration response has been effectively reduced by setting bearings only for relatively high earthquake intensity. Compared with LRB and SRB, SLRB works with more compositive seismic isolation effect. The "slide" action of the telflon-stainless-steel interface in SLRB can significantly reduce the acceleration response of girder, while the relative displacement between the pier and girder for this novel bearing is not increased due to the occurrence of collision in the bearing.

Keywords: girder bridge; seismic isolated; shaking table test slide and collision; sliding lead rubber bearing

1. Introduction

In the past decades, there have been many major earthquakes around the world. The lessons learned from major earthquakes show that the traffic disruption caused by the collapse of bridges may greatly aggravate the property damage and casualties. In order to improve the seismic performance of structures, researchers have proposed new seismic technologies, including passive control, active control, hybrid control, etc., among which the seismic isolation technology is to separate structure from ground shaking by installing isolation devices, and subsequently reduce the seismic energy transmitted to the upper structure. For concrete girder bridges, the isolation device is mainly installed between the lower pier and the upper girder, and the natural vibration period of bridge is extended to greatly reduce the acceleration response of girder.

In recent years, researchers have carried out systematic experimental investigation and numerical simulation on seismic response of bridges with different bearings. Tsopelas *et al.* (1996) combined sliding bearing with metal damper and studied the seismic mitigation effect for bridges by shaking table tests. Chaudhary *et al.* (2001) utilized recorded seismic data of base-isolated Yama-agé bridge to identify material parameters of high damping rubber bearings, and then

---

∗Corresponding author, Assistant Professor, E-mail: wuyifeng@bucea.edu.cn

developed corresponding numerical model to analyze the foundation soil interaction. Shen *et al.* (2004) verified the accuracy of the established Bai-Ho isolated bridge model based on environmental vibration data, and discussed the influence of two types of simulated near-fault pulses on the seismic response of the bridge. Jangid (2004) conducted experiment on a three-span continuous girder bridge that seismic isolated with lead rubber bearings (LRB), results show that the biaxial coupling effect of the bearing has a significant impact on seismic responses of the bridge. Kunde and Jangid (2006) found the stiffness of both the main girder and the pier has few impacts on the dynamic properties of seismic isolated bridges. Dicleli *et al.* (Dicleli and Buddaram 2006, Dicleli 2007) compared the seismic mitigation effect of different isolation schemes, and discussed the response characteristics of seismic isolated bridges when subjected to near-fault earthquakes. Tsai *et al.* (2007) studied the seismic response of the roller-supported seismic isolated bridge, and proposed a prediction formula for the maximum acceleration response of the main girder. Li *et al.* (2008) proposed two shape-memory-alloy devices and investigated the seismic mitigation mechanism of them by experiment and numerical simulation. Based on the parallel computing package, ADVENTURE Cluster, Ohsaki *et al.* (2009, 2015) developed a numerical model for a seismic isolated frame by using solid elements, the number of degrees of freedom exceeded 3 million, and the calculation results were verified by full scale model test. Sahasrabudhe and Nagarajaiah (2010) presented a combination of sliding bearing and magneto-rheological damper to reduce seismic responses, and modified the motion equation by adding the MR damper force. Filipov *et al.* (2013) carried out longitudinal and lateral pushover analysis of a girder bridge, in which the laminated rubber bearing combined with elastoplastic block were used to realize seismic isolation. Eröz and DesRoches (2013) established an improved model to consider the effects of vertical load, biaxial coupling and large deformation of friction pendulum bearing. Xiang and Li (2017) systematically studied the hysteretic behaviors of the laminated rubber bearing under different surface pressures and different loading rates, and discussed the seismic sliding mechanism of the bearing for girder bridges during moderate-to-major earthquakes. Ponzo *et al.* (2017) analyzed the restoring capability of the double concave friction pendulum, and discussed the formula of the maximum residual displacement given by previous studies. Wu *et al.* (2017, 2018) conducted numerical simulations of a sliding lead rubber bearing (SLRB) based on explicit finite element method and conducted experimental verification. Zheng *et al.* (2021) combined the friction pendulum bearing and the shape-memory-alloy wire to form a new isolation system, and explored the influence of different design parameters of the system on the seismic mitigation effect of bridge.

The above literature review indicates that systematic numerical simulation and experiment have been conducted to uncover the isolation mechanism of girder bridges. At present, researches mainly focus on investigating new seismic isolation devices, and exploring the seismic isolation mechanism of these devices by experiment and numerical simulation. In this study, a novel type of SLRB proposed by previous researches (Xing *et al.* 2012, Wu *et al.* 2017), as well as the lead rubber bearing and sliding rubber bearing (SRB) with the same size, were briefly introduced. Then, a girder bridge with a 1/4 scale ratio was fabricated, and the shaking table tests of the bridge that isolated by the above three types of bearings were carried out. The objective of this study is to find out the isolation mechanism of the new type of bearing, and compare its seismic mitigation effect with the other two types of bearings.
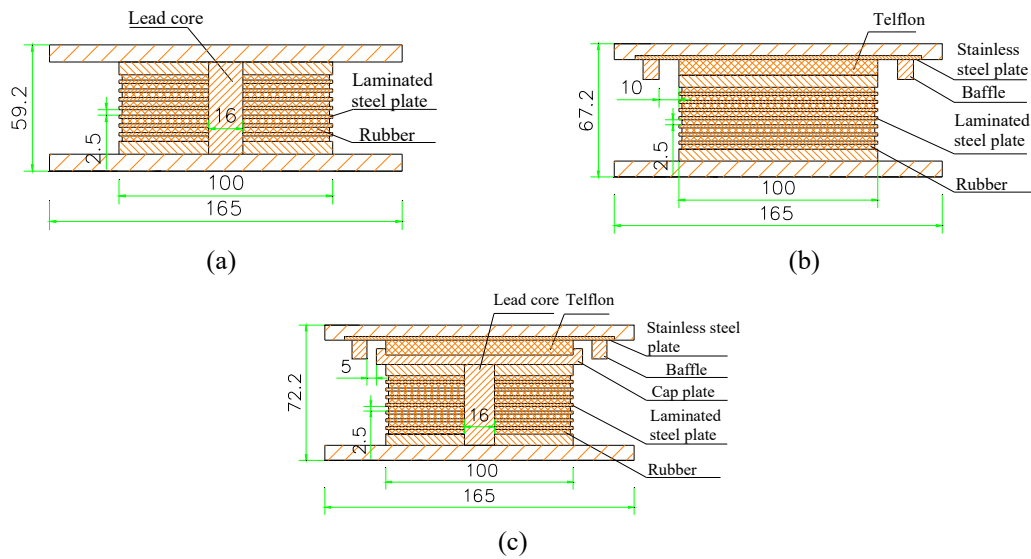
Fig. 1 Conformation of bearings (unit: mm): (a) LRBl; (b) SRB; (c) SLRB

2. Bearings

The SLRB consists of the upper sliding device and the lower LRB, the diameter of the bearing is 100 mm, the gap between the baffle and the cap plate is 5 mm, the thickness of the laminated rubber plate is 2.5 mm, the shear modulus of rubber is 0.8 MPa. The design parameters of the other two bearings, like the diameter, the thickness of rubber and steel plate, are the same with those of SLRB. More details about the three types of bearings can be obtained from Fig. 1.

In previous studies (Wu *et al.* 2017, 2018), the working principle of the above three bearings were explicated, and the corresponding experimental researches have been conducted to investigate the mechanical properties of these bearings. Taking the novel SLRB as an example, it is a combination of SRB and LRB, which allows the displacement of bridges caused by temperature, concrete creep under normal conditions, and has better seismic isolation effect when

Fig. 2 Loading equipment
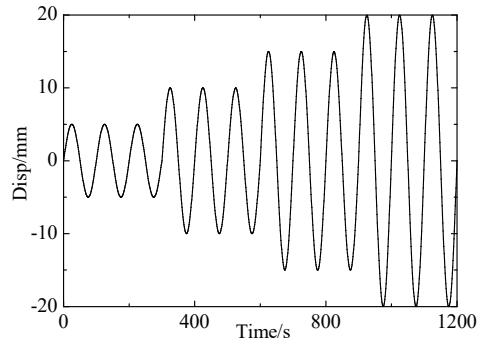
Fig. 3 Loading scheme

(a)

(b)

(c)
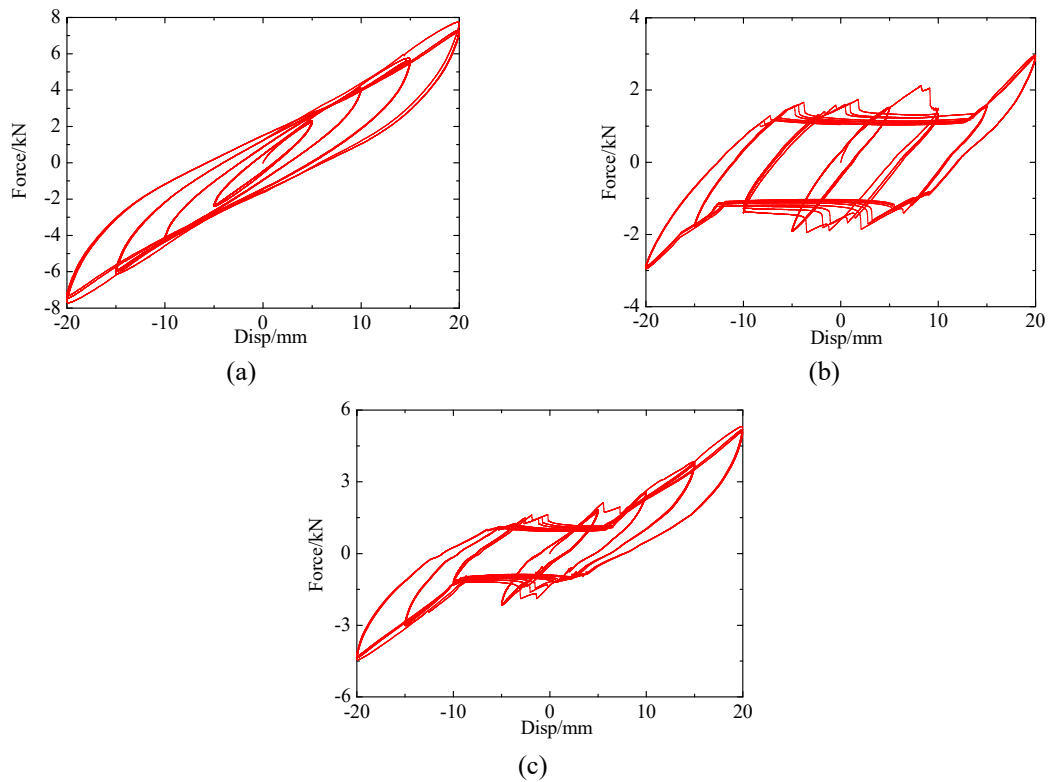
Fig. 4 Hysteresis curve of bearings: (a) LRB; (b) SRB; (c) SLRB

moderate and major earthquake occurs. For the experiment of these bearings, the loading equipment and scheme are shown in Figs. 2 and 3. The vertical pressure of bearings is determined as 25.5 kN to be in accordance with the following shaking table tests. The loading rate of the compression-shear test is 0.01 Hz, the maximum shear displacement of each circle is set as 5 mm, 10 mm, 15 mm and 20 mm and repeated by three times. The corresponding mechanical results are illustrated in Fig. 4. It can be seen the hysteresis curves of SLRB integrates the above mentioned "slide" feature of SRB and the "post-yield stiffening" of LRB as the displacement is lower and

higher than 5 mm, and in the displacement range from -20 mm to 20 mm, the equivalent horizontal stiffness of the three bearings can be sorted as SRB < SLRB < LRB.

Fig. 5 Elevation of the bridge

Fig. 6 Bearing in the bridge

Ⓐ : Accelerometer

Ⓓ : Displacement sensor
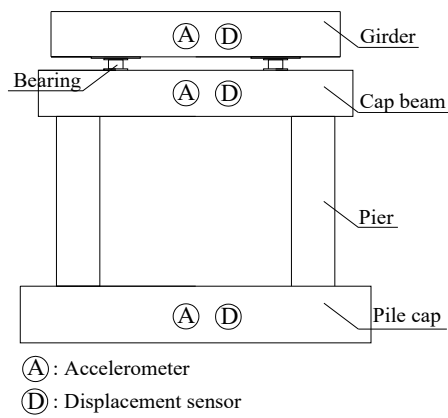
Fig. 7 Sensor arrangement

Table 1 Scaling factors of parameters

Parameters	Scaling factors	Scaled model	Parameters	Scaling factors	Scaled model
Length	λ_l	1/4	Time	$\lambda_T = \lambda_L \sqrt{\dfrac{\lambda_{\rho_e}}{\lambda_E}}$	$1/2\sqrt{2}$
Equivalent density	λ_ρ	2	Displacement	λ_l	1/4
Modulus	λ_E	1	Acceleration	$\lambda_a = \lambda_E/(\lambda_L \lambda_{\rho_e})$	2

3. Bridge model

As shown in Fig. 5, a simply-supported bridge model with a 1/4 geometric scaling factor of the proto-type bridge was designed and fabricated, it consists of a concrete rectangular girder and two piers. The span length and width of the girder are 4 m and 2 m, the mass of the girder is 10.4 ton. Each pier is composed of two circular columns with the diameter being 0.3 m and a 2.15 m cap beam in length. Fig. 6 shows the above bearings installed on the top of cap beam to isolate girder, there are all four bearings in the bridge model. The bottom of the model is the rigid pile cap, it is fixed to the shaking table to realize a rigid boundary condition. According to the similarity rule, the scaling factors of parameters are presented in Table 1. Besides, as illustrated in Fig. 7, three accelerometers and three displacement sensors are set to acquire the seismic response of the bridge.

4. Shaking table tests of the bridge model

As shown in Fig. 8, three Chinese-seismic-code-compatible records revised by the software, Seismo-Match (Hancock *et al*. 2006), are utilized as input to investigate the seismic performances of the bridge isolated with different bearings, the time series of records are compressed by a scale factor $2\sqrt{2}$. Fig. 9 shows the response spectra of the records with 5% elastic damping ratio, in

(a)   (b)

(c)
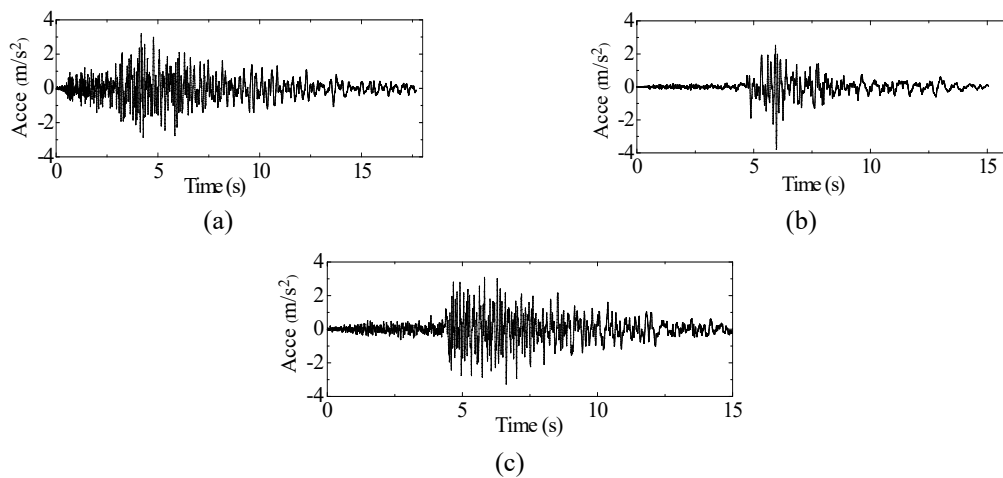
Fig. 8 Earthquake records: (a) I wave; (b) II wave; (c) III wave
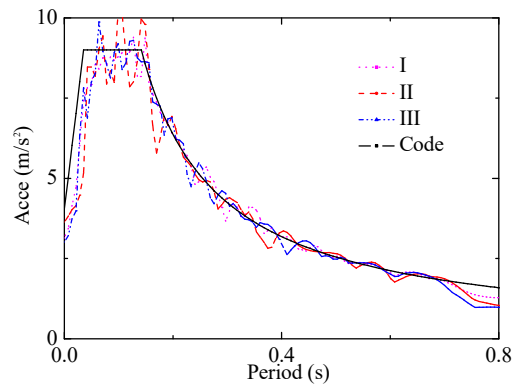
Fig. 9 Response spectra of records

which the code spectra is determined by setting the peak acceleration 0.4 g. After the earthquake records revised by the above-mentioned software, it can be seen the response spectra of the three records are all consistent with the code spectra, even though the peak ground acceleration (PGA) of each record is a bit lower than 0.4 g. So, the PGA of each record in Fig. 8 is deemed as "equivalent 0.4 g" below. In the shaking table test, the white noise (WN) excitation and the above three records with the PGA value gradually increasing are input along longitudinal direction to investigate the dynamic characteristics and seismic behavior of the bridge model, the input sequence of records is shown as follows, WN(0.01 g) → I/II/III(0.05 g) → WN(0.01 g) → I/II/III(0.1 g) → …… → I/II/III(0.35 g) → WN(0.01 g) → I/II/III(0.4 g) → WN(0.01 g).

5. Test results

5.1 Dynamic characteristics

Fig. 10 shows the variation of primary frequency of the bridge after inputting the above records with different intensities. It is noted that the primary frequency decreases gradually with the increase of PGA, indicating that the dynamic characteristics of the bridge has been changed through loading schemes of different PGA values. Moreover, the frequency of the bridge equipped with SRB is obviously much smaller than those equipped with SLRB and LRB, the reason mainly lies in the lead core in the latter two bearings. Although the frequency decreases gradually, which usually means the damage in the bridge, no obvious cracks are found on the pier or the girder during the whole test.

5.2 Acceleration response

5.2.1 Response of different parts of the bridge
Taking the III wave with the equivalent PGA 0.4 g as an example, the acceleration responses of different parts in the bridge are shown in Fig. 11. It is noted that the cap beam's peak acceleration response is always about 2 times of that of the pile cap, while the corresponding response of the girder is much lower than the cap beam. This phenomenon mainly results from setting rubber bearings, and the lateral stiffness of bearings is much less than piers. However, it should be
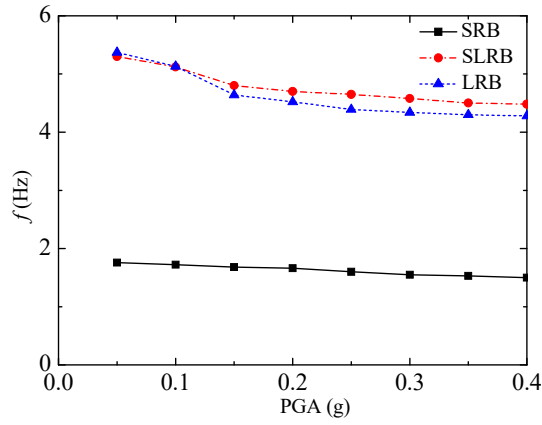
Fig. 10 Variation of primary frequency

(a)

(b)

(c)
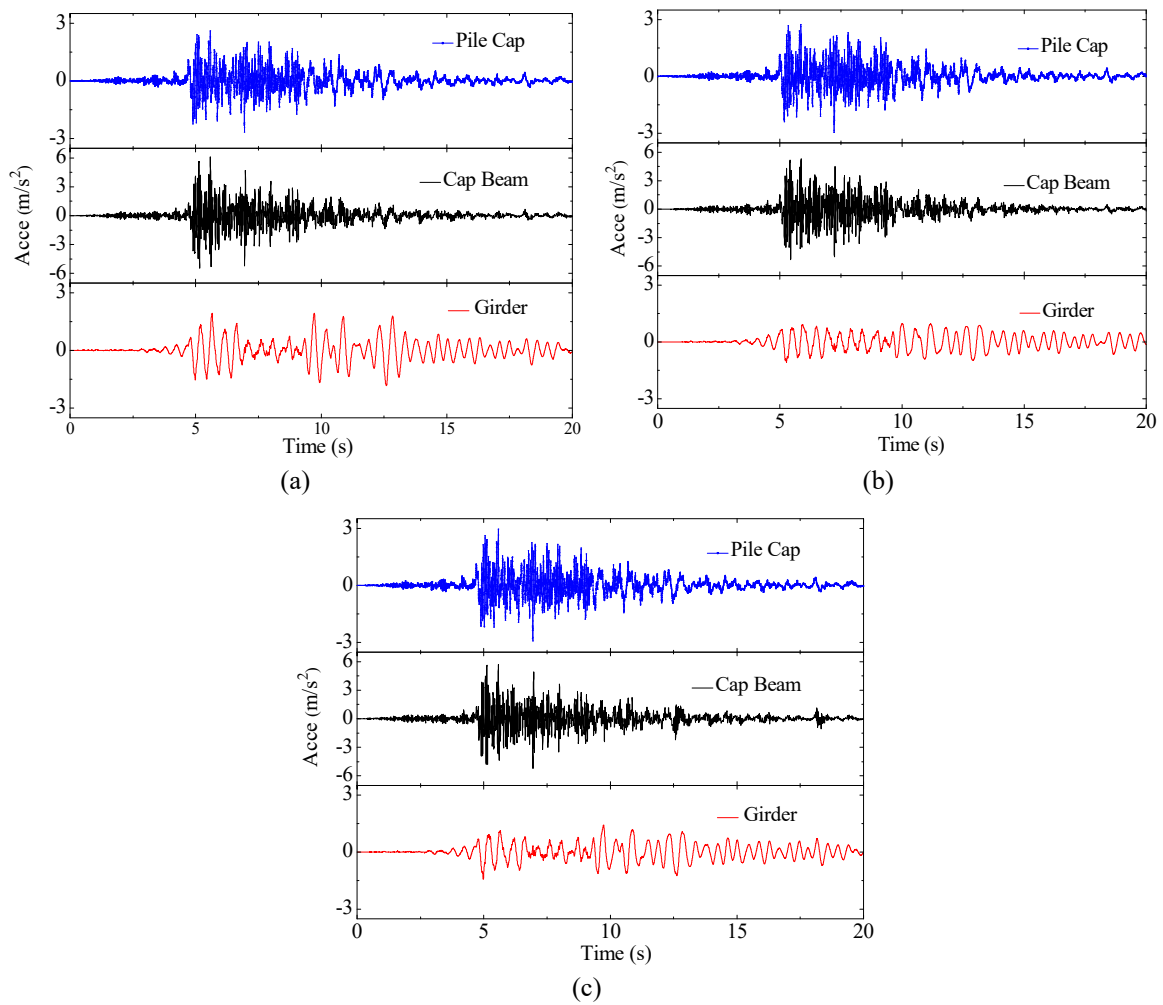
Fig. 11 Response of different parts of the bridge: (a) LRB; (b) SRB; (c) SLRB

mentioned that the acceleration response of the girder is not always mitigated throughout the record input, an obvious exception can be observed when time exceeds 12.5 s, which indicates the girder response has been amplified compared with that of the pile cap as the earthquake intensity is small. In addition, the dominant frequency of the acceleration response of the girder is obviously lower than that of the pile cap and the cap beam. For the influences of different types of bearings, the girder's seismic response in Fig. 11(a) that using LRB in the bridge is the largest, the peak value of the girder's response in Fig. 11(b) is about half of that in Fig. 11(a). Besides, due to the energy consumption of the lead core, the acceleration response of the girder in Figs. 11(a) and 11(c) has a significant attenuation effect, while this effect is not remarkable for the bridge isolated by SRB.

5.2.2 Correlation between the girder's response and PGA

As mentioned above, the equivalent PGA of each record used in the shaking table test increased from 0.05 g to 0.4 g with an equal interval, 0.05 g. Taking the II wave as an example, the acceleration responses of the girder with the above three different types of bearings are presented in Fig. 12. For simplification, only the results with PGA being 0.1 g, 0.2 g, 0.3 g and 0.4 g are included.
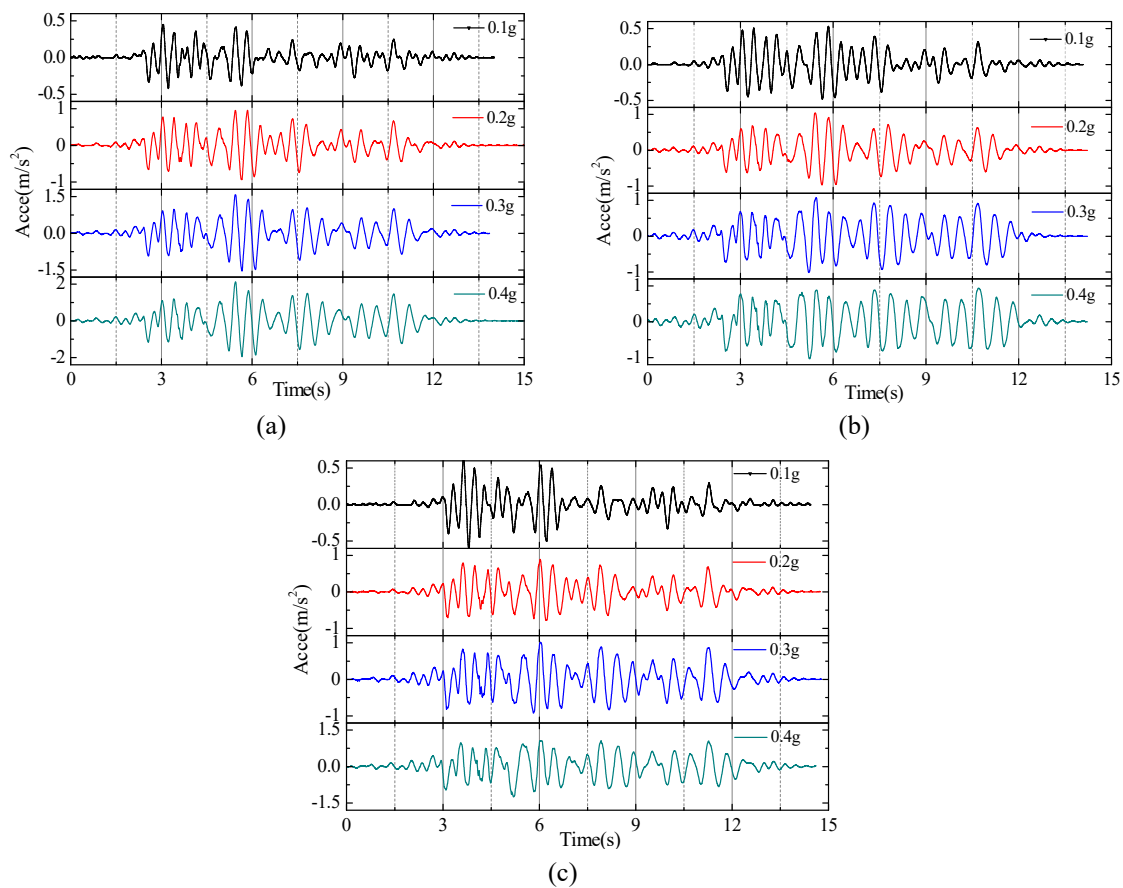
Fig. 12 The girder's acceleration time histories with different PGA values: (a) LRB; (b) SRB; (c) SLRB

As can be seen from Fig. 12, the response of the girder is closely correlated with the PGA of the input record and the type of bearing. The detailed performance is demonstrated as follows: (1) When using the LRB, the acceleration response increases nearly linearly with the PGA value, the shape of the acceleration time history is almost unchanged with only some local differences. (2) When using SRB, the response of the girder only increases within the range of 0.1 g-0.2 g, and then it no longer increases and even tends to decrease. (3) When the SLRB is adopted, the variation of acceleration response is similar to that of LRB in the range of 0.1 g-0.2 g, as the PGA value is 0.3 g, the response does not increase significantly, but it increases again when the peak value reaches 0.4 g.

In order to more intuitively reflect the connection between the acceleration response of the girder and the equivalent PGA, the variation of the acceleration response for different types of bearings are illustrated in Fig. 13. It clearly shows the response of the girder isolated by SLRB is a compromise of those of LRB and SRB. Based on the results in Fig. 13, the ratio calculated by dividing the girder's peak acceleration value of SLRB with that of SRB, abbreviated as SLRB/SRB, and the ratio, SLRB/LRB, are obtained and presented in Fig. 14. As shown in Fig. 14, the ratio, SLRB/LRB, fluctuates around 1.0 as the PGA is less than 0.2 g, indicating a little difference between the peak acceleration results, then this ratio is positively correlated with PGA,
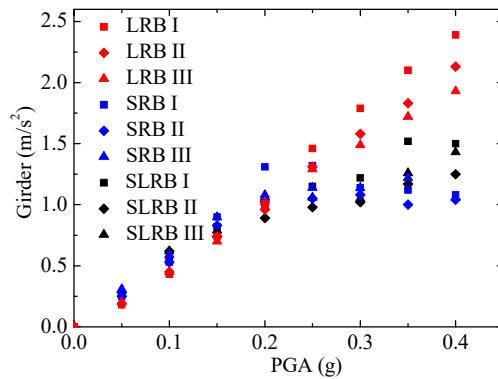
Fig. 13 The girder's peak acceleration response
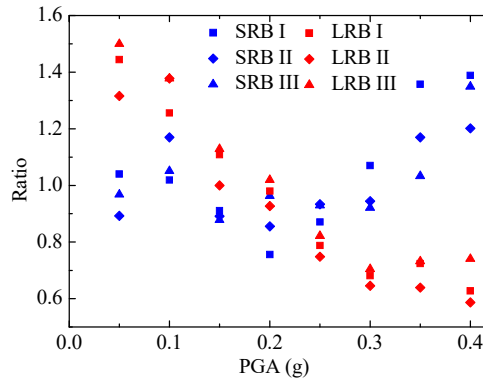
Fig. 14 Ratio of acceleration response

namely, the acceleration response of the SLRB-isolated girder is greater than that of SRB-isolated girder, which is directly determined by the horizontal stiffness of the two bearings. On the other hand, the ratio of SLRB/LRB decreases from 1.5 to 0.7 with the increase of PGA, which is mainly due to the "slide" action in the SLRB. In general, for low earthquake intensity, the greater stiffness of the bearing will result in the smaller acceleration response of the girder, as the intensity increases, the conclusion is just opposite.

5.3 Displacement response

The relative displacement between the girder and the pier, namely the shear displacement of bearing, is an important index to measure the displacement response of seismic isolated bridge. In this section, the peak relative displacement between the girder and the pier for different bearings are presented in Fig. 15, and the ratio of relative displacement response is shown is Fig. 16.

As shown in Fig. 15, there is a positive correlation between the peak relative displacement and the PGA value of earthquake records for LRB, SRB and SLRB. When PGA is no more than 0.15 g, the value of shear displacement for different bearings are all less than 5mm, and can be sorted as SRB > SLRB > LRB, which directly results from the horizontal shear stiffness of bearings. When
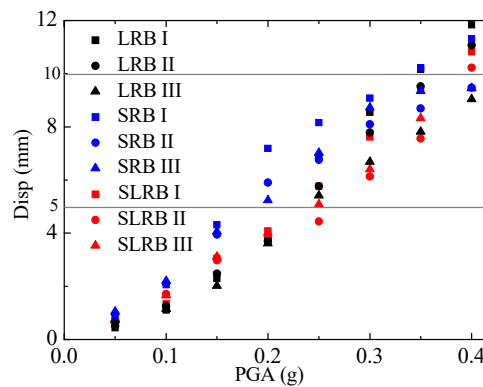
Fig. 15 The peak relative displacement response
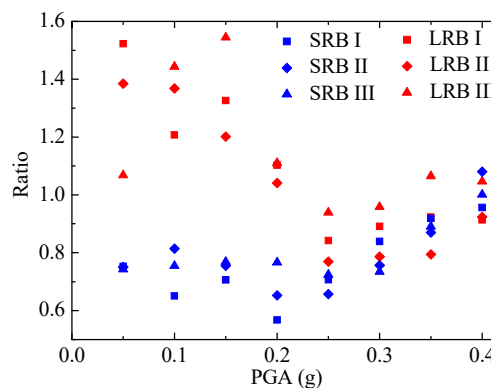
Fig. 16 Ratio of relative displacement response

PGA is in the range from 0.2 g to 0.3 g, the displacement response of SRB is still the largest, but the displacement of LRB increases more rapidly than SLRB, and the sequence changes to SRB > LRB > SLRB as the PGA is 0.3 g. Within this range, the collision between the upper baffle and the lower LRB of the SLRB occurs, and the sound of banging is also heard in the shaking table test. With the further increase of PGA, the collision also appears for SRB, no obvious relation of the displacement for the three types of bearings can be determined according to Fig. 15.

Fig. 16 shows the displacement of SLRB is always a bit lower than that of SRB, and is also less than that of LRB as the PGA being in the range from 0.25 g to 0.4 g. Generally speaking, the occurrence of collision reduces the displacement response of the bearing to a certain extent, and for relatively high earthquake intensity, the displacement response of SLRB does not show an obvious amplification compared with that of LRB.

6. Conclusions

In the present study, a novel sliding lead rubber bearing (SLRB) integrates the features of lead rubber bearing (LRB) and sliding rubber bearing (SRB) is introduced, the mechanical properties of the novel bearing are investigated by experiment. Then, a 1/4 scaled simply supported bridge is fabricated, the dynamic characteristics and seismic response of the bridge seismic isolated respectively by SLRB, SRB and LRB are further studied. Some conclusions are drawn as follows.

- The primary frequency of the SRB-isolated bridge is much smaller than those of SLRB-isolated and LRB-isolated bridge. With the increase of earthquake intensity, the frequency of the bridge decreases gradually even though no obvious cracks are found on the pier or the girder.
- The peak acceleration response of the cap beam is about 2 times of that of the pile cap, while the peak value of the girder is much smaller than that of the cap beam. However, it is found the seismic isolated bridge shows no seismic mitigation effect as the earthquake intensity is low, no matter what type of the bearing is.
- Compared with LRB, the acceleration response of SLRB-isolated bridge is significantly reduced for relatively high earthquake intensity, which is mainly due to the "slide" action in the telflon-stainless steel interface.
- Compared with LRB, the displacement response of SLRB is a bit smaller as the PGA being in the range from 0.25 g to 0.4 g, which mainly results from the collision between the upper baffle and the lower LRB. Besides, it is always smaller than that of SRB in the whole range of PGA.

In the subsequent research, we will consider using the new bearing in building structures and other types of bridges to conduct shake table tests, which can further investigate the performance of the bearing when used in buildings and bridges.

References

Chaudhary, M.T.A., Abe, M. and Fujino, Y. (2001), "Performance evaluation of base-isolated Yama-agé bridge with high damping rubber bearings using recorded seismic data", *Eng. Struct.*, **23**(2), 902-910. https://doi.org/10.1016/S0141-0296(00)00117-6

Dicleli, M. (2007), "Supplemental elastic stiffness to reduce isolator displacements for seismic-isolated bridges in near-fault zones", *Eng. Struct.*, **29**(5), 763-775. https://doi.org/10.1016/j.engstruct.2006.06.013

Dicleli, M. and Buddaram, S. (2006), "Effect of isolator and ground motion characteristics on the performance of seismic-isolated bridges", *Earthq. Eng. Struct. D*, **35**(2), 233-250. https://doi.org/10.1002/eqe.522

Eröz, M. and DesRoches, R. (2013), "A comparative assessment of sliding and elastomeric seismic isolation in a typical multi-span bridge", *J. Earthq. Eng.*, **17**(5), 637-657. https://doi.org/10.1080/13632469.2013.771589

Filipov, E.T., Fahnestock, L.A., Steelman, J.S., Hajjar, J.F., LaFave, J.M. and Foutch, D.A. (2013), "Evaluation of quasi-isolated seismic bridge behavior using nonlinear bearing models", *Eng. Struct.*, **49**(2), 168-181. https://doi.org/10.1016/j.engstruct.2012.10.011

Hancock, J., Watson-Lamprey, J., Abrahamson, N.A., Bommer, J.J., Markatis, A., Mccoy, E. and Mendis, R. (2006), "An improved method of matching response spectra of recorded earthquake ground motion using wavelets", *J. Earthq. Eng.*, **10**(1), 67-89.

Jangid, R.S. (2004), "Seismic response of isolated bridges", *J. Bridge Eng.*, **9**(2), 156-166. https://doi.org/10.1061/(ASCE)1084-0702(2004)9:2(156)

Kunde, M.C. and Jangid, R.S. (2006), "Effects of pier and deck flexibility on the seismic response of isolated bridges", *J. Bridge Eng.*, **11**(1), 109-121. https://doi.org/10.1061/(ASCE)1084-0702(2006)11:1(109)

Li, H., Mao, C.X. and Ou, J.P. (2008), "Experimental and theoretical study on two types of shape memory alloy devices", *Earthq. Eng. Struct. D*, **37**(3), 407-426. https://doi.org/10.1002/eqe.761

Ohsaki, M., Miyamura, T., Kohiyama, M., Hori, M., Noguchi, H., Akiba, H., Kajiwara, K. and Ine, T. (2009), "High-precision finite element analysis of elastoplastic dynamic responses of super-high-rise steel frames", *Earthq. Eng. Struct. D*, **38**(5), 635-654. https://doi.org/10.1002/eqe.900

Ohsaki, M., Miyamura, T., Kohiyama, M., Yamashita, T., Yamamoto, M. and Nakamura, N. (2015), "Finite-element analysis of laminated rubber bearing of building frame under seismic excitation", *Earthq. Eng. Struct. D*, **44**(11), 1881-1898. https://doi.org/10.1002/eqe.2570

Ponzo, F.C., Cesare, A.D., Leccese, G. and Nigro, D. (2017), "Shake table testing on restoring capability of double concave friction pendulum seismic isolation systems", *Earthq. Eng. Struct. D*, **46**(14), 2337-2353. https://doi.org/10.1002/eqe.2907

Sahasrabudhe, S.S. and Nagarajaiah, S. (2010), "Semi-active control of sliding isolated bridges using MR dampers: an experimental and numerical study", *Earthq. Eng. Struct. D*, **34**(8), 965-983. https://doi.org/10.1002/eqe.464

Shen, J., Tsai, M.H., Chang, K.C. and Lee, G.C. (2004), "Performance of a seismically isolated bridge under near-fault earthquake ground motions", *J. Struct. Eng.*, **130**(6), 861-868. https://doi.org/10.1061/(ASCE)0733-9445(2004)130:6(861)

Steelman, J.S., Fahnestock, L.A., Filipov, E.T. and LaFave, J.M. (2013), "Shear and friction response of nonseismic laminated elastomeric bridge bearings subject to seismic demands", *J. Bridge Eng.*, **18**(7), 612-623. https://doi.org/10.1061/(ASCE)BE.1943-5592.0000406

Tsai, M.H., Wu, S.Y., Chang, K.C. and Lee, G.C. (2007), "Shaking table tests of a scaled bridge model with rolling-type seismic isolation bearings", *Eng. Struct.*, **29**(5), 694-702.

https://doi.org/10.1016/j.engstruct.2006.05.025

Tsopelas, P., Constantinou, M.C., Okamoto, S., Fujii, S. and Ozaki, D. (1996), "Experimental study of bridge seismic sliding isolation systems", *Eng. Struct.*, **18**(4), 301-310. https://doi.org/10.1016/0141-0296(95)00147-6

Wu, Y.F., Wang, H., Li, A.Q., Feng, D.M., Sha, B. and Zhang, Y.P. (2017), "Explicit finite element analysis and experimental verification of a sliding lead rubber bearing", *J. Zhejiang Uni. SCI. A*, **18**(5). 363-376. https://doi.org/10.1631/jzus.A1600302

Wu, Y.F., Wang, H., Sha, B., Zhang, R.J. and Li, A.Q. (2018), "The compression-shear properties of small-size seismic isolation rubber bearings for bridges", *Struct. Monitor. Maint., Int. J.*, **5**(1) 39-50. https://doi.org/10.12989/smm.2018.5.1.039

Xiang, N. and Li, J. (2017), "Experimental and numerical study on seismic sliding mechanism of laminated-rubber bearings", *Eng. Struct.*, **141**(8), 159-174. https://doi.org/10.1016/j.engstruct.2017.03.032

Xing, C.X., Wang, H., Li, A.Q. and Wu, J.R. (2012), "Design and experimental verification of a new multi-functional bridge seismic isolation bearing", *J. Zhejiang Uni. SCI. A*, **13**(12), 904-914. https://doi.org/10.1631/jzus.A1200106

Zheng, W.Z., Wang, H., Li, J. and Shen, H.J. (2021), "Parametric study of SMA-based friction pendulum system for response control of bridges under near-fault ground motions", *J. Earthq. Eng.*, **25**(8), 1494-1512. https://doi.org/10.1080/13632469.2019.1582442

Zhou, T., Wu, Y.F. and Li, A.Q. (2018), "Numerical study on the ultimate behavior of elastomeric bearings under combined compression and shear", *KSCE J. Civil Eng.*, **22**(9), 3556-3566. https://doi.org/10.1007/s12205-018-0949-y

CC